Central European Journal of Energetic Materials, **2013**, *10*(1), 123-133
ISSN 1733-7178

Preparation of Al Nanoparticles and Their Influence on the Thermal Decomposition of RDX

Conghua HOU[1], Xiaoheng GENG[2], Chongwei AN[1*], Jingyu WANG[1], Wenzheng XU[1] and Xiaodong LI[1]

[1] *Chemical Industry and Ecology Institute, North University of China, Taiyuan Shanxi, 030051, China*
[2] *Urban and Environmental Science Department, Binzhou University, Binzhou, Shandong 256600, China*
[*] *E-mail*: *anchongwei@yahoo.cn*

Abstract: Aluminum (Al) nanoparticles were prepared by the DC arc plasma method in order to study the influence of Al nanoparticles on the thermal decomposition of cyclotrimethylenetrinitramine (RDX). The Al powder was characterized by TEM, BET, XRD, and LSA, and the thermal decomposition of RDX and RDX/nanometer Al were examined by DSC. Based on the DSC curves, the thermal decomposition parameters of the samples were calculated and compared. The results showed that the particles of Al are homogeneous and fine, and that the surface is smooth. The TEM results showed that the nanoparticles are spherical, with an average diameter of approximately 60 nm. The peak temperature of RDX decomposition decreased by 4.36 K at the heating rates of 5, 10, and 20 K/min after the addition of nano-Al powder, and the activation energy for decomposition decreased by about 11 kJ/mol. Furthermore, the critical explosion temperature was also reduced. These observable changes indicate that Al nanoparticles act as catalysts for the thermal decomposition of RDX.

Keywords: Al nanoparticles, properties, RDX, thermal decomposition

Introduction

Nano powders, such as nano metals, nano metal oxides, and nano explosive particles, have been studied and used in the energetic materials field because of their large specific surface areas and outstanding properties [1-4]. These

nanoparticles are not only effective for improving the combustion rate or detonation velocity of energetic materials, but also for improving the heat of detonation and blast characteristics [5-7]. From these improvements, it can be inferred that nanoparticles allow energetic materials to decompose more completely. Moreover, nanosized metal and metal oxide particles have been proven to be effective in improving the decomposition or explosion of ammonium perchlorate (AP), the main energetic filler and common oxidizer in composite solid propellants [8-11].

Aluminum (Al) powder, a common ingredient in energetic materials formulations, can improve energy, ignition, and combustion performance. Al is often added to organic (CHON) explosives to improve their blast force because Al can liberate an amount of energy several times greater than that of organic high explosives [12]. Aluminized explosives have been studied for several years and have exhibited numerous outstanding properties [13-15]. In the early 1980s, Reshetov et al. [16] found that Al nanoparticles enhanced the detonation rate of cyclotrimethylenetrinitramine (RDX). More recently, a beneficial enhancement has been demonstrated [17-20] of both detonation velocity and brisance for explosives containing Al nanoparticles. However, the influence of nanoparticles on the thermal decomposition of organic explosives has not been investigated and thoroughly understood. In this study, Al nanoparticles were prepared by the DC arc plasma method and their effect on the thermal decomposition of an organic explosive, RDX, was tested and analyzed.

Experimental

Materials

Al rod (purity>99.5%) was purchased from the Aluminum Corporation of China. RDX was provided by Xi'an Modern Chemistry Research Institute of China. Hydrogen (purity>99%) and Argon (purity>99%) were purchased from Taigang of China.

Preparation of Al nanoparticles

Al nanoparticles were prepared using the SNH-IV-B plasma equipment (SiPing Gao Sida Nanomaterial & Equipment Co., Ltd, China). A schematic of the experimental equipment is shown in Figure 1. Firstly, the Al rod was placed in a Cu crucible in the work chamber, which was evacuated to 0.09 MPa by the vacuum pump. Secondly, the protective gases, 40% Hydrogen and 60% Argon, were introduced into the work chamber until the chamber pressure was 1 atm.

Thirdly, the positive and negative electrodes were charged; a stable arc plasma was formed between the two electrodes. The Al rod melted and evaporated to form metal vapor under the influence of the high-temperature plasma. Al recrystallized from the metal vapor and became Al nanoparticles when the metal vapor was channelled towards the cooling area. After the arc had been switched off, the system was passivated in an Ar atmosphere for 24 h and then further passivated by the introduction of a few atmospheres (1.013×10^5 Pa). Finally, collected the Al nanoparticles.

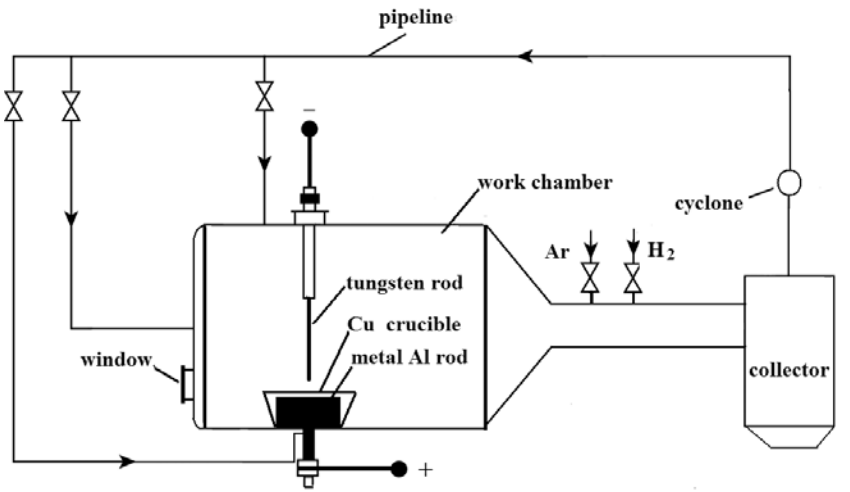

Figure 1. Schematic diagram of the experimental equipment.

Characterization of Al nanoparticles

The particle size of the Al powder was measured using a JEM-2010 High Resolution Transmission Electron Microscope (HRTEM; JEOL Co., Japan). X-ray diffraction (XRD) was carried out with a Rigaku D/MAX2550 VB+/PC (Japan) in order to ascertain the crystal structure of the sample. The surface area of the Al nanoparticles was measured using a BET specific surface area tester. Granularity was characterized using a BI-90PLUS Laser Sizer (Brookhaven Instruments Co., USA).

Preparation of the mixture of RDX and Al nanoparticles

RDX (9 g) and Al nanoparticles (1 g) were added to ethanol (20 ml) and dispersed by ultrasonication for a few minutes. The samples were then dried under vacuum. Finally, the powder mixtures were milled for 10 min prior to being homogenized.

DSC test

The DSC experiments on RDX and the mixtures of RDX and Al nanoparticles were carried out using a DSC131 instrument (Setaram Co., France). The DSC conditions were as follows: sample mass, 0.7 mg; heating rate, 5, 10, and 20 K/min; N_2 atmosphere (30 ml/min).

Results and Discussion

TEM analysis

The Al nanoparticles prepared via the plasma method were characterized by TEM (Transmission Electron Microscope); the results are shown in Figure 2.

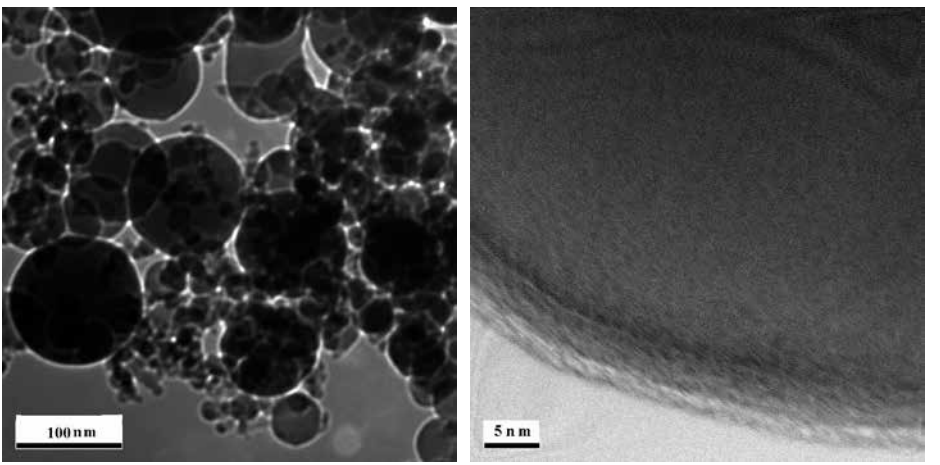

Figure 2. TEM images of Al nanopowder.

The morphology of the Al nanoparticles was spherical, with a particle size of approximately 40 nm to 80 nm, as shown in Figure 2a. The nanoparticles agglomerated because of their high surface energy and magnetic property. The high magnification TEM image in Figure 2b indicates that a dense film, thickness 4 nm, is evenly coated on the surface of the Al nanoparticles. This was identified as the oxide.

BET analysis

The BET (acronym of scientists' names: Brunauer, Emmett and Teller) surface area (S_W) of the Al nanoparticles was determined to be 36.57 m^2/g by the multilayer gas adsorption method. According to Equation 1 [21], the average

size of the Al nanoparticles was 61 nm. This result is in agreement with the TEM results.

$$d=6/(\rho \cdot S_W) \quad (1)$$

where d is the particle diameter in m; S_W is the BET surface area in m^2/g; and ρ is the density of the Al particles in $kg.m^{-3}$.

XRD characterization

XRD (X-ray Diffraction) was employed for testing the Al nanoparticles; the results are shown in Figure 3.

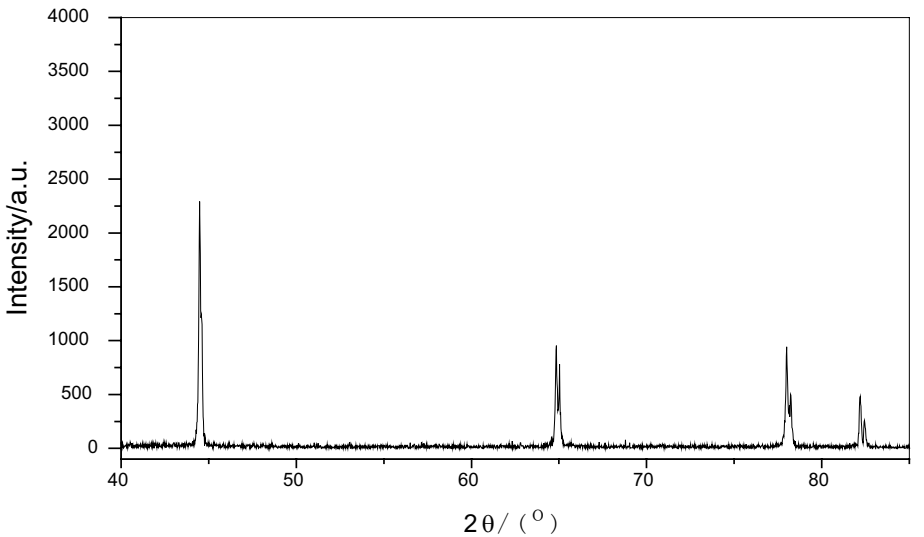

Figure 3. XRD pattern for Al nanoparticles.

Figure 3 shows that the peaks of Al nanoparticles are all very intense. The diffraction data are in good agreement with the Joint Committee on Powder Diffraction Standards (JCPDS) card for Al. Following the Scherrer equation [22], the crystal size of the Al nanoparticles was calculated to be 59 nm**.**

LSA analysis

The LSA (Laser Size Analysis) of the samples is shown in Figure 4.

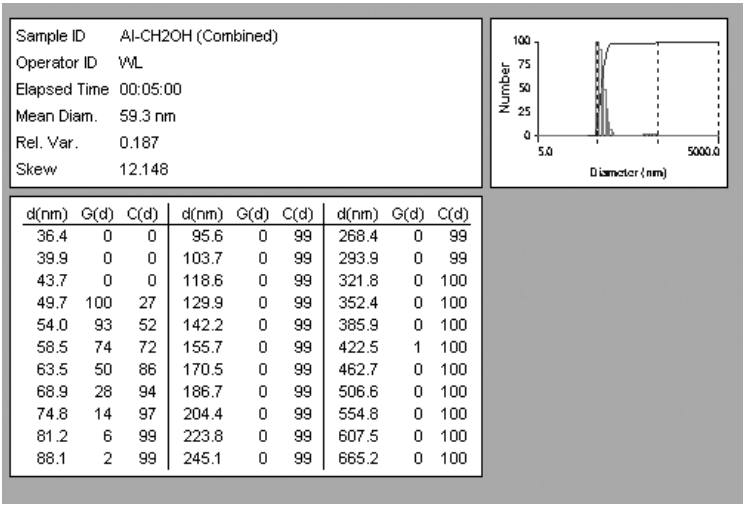

d(nm)	G(d)	C(d)	d(nm)	G(d)	C(d)	d(nm)	G(d)	C(d)
36.4	0	0	95.6	0	99	268.4	0	99
39.9	0	0	103.7	0	99	293.9	0	99
43.7	0	0	118.6	0	99	321.8	0	100
49.7	100	27	129.9	0	99	352.4	0	100
54.0	93	52	142.2	0	99	385.9	0	100
58.5	74	72	155.7	0	99	422.5	1	100
63.5	50	86	170.5	0	99	462.7	0	100
68.9	28	94	186.7	0	99	506.6	0	100
74.8	14	97	204.4	0	99	554.8	0	100
81.2	6	99	223.8	0	99	607.5	0	100
88.1	2	99	245.1	0	99	665.2	0	100

Figure 4. LSA distribution drawing of the Al nanoparticles.

The mean diameter of the samples was 59.3 nm. The granularity distribution was uniform, in agreement with the results from the TEM and BET analyses.

Results of thermal analysis

Figure 5 shows the DSC thermographs of RDX and the mixture of RDX with Al nanoparticles at heating rates of 5, 10, and 20 K/min.

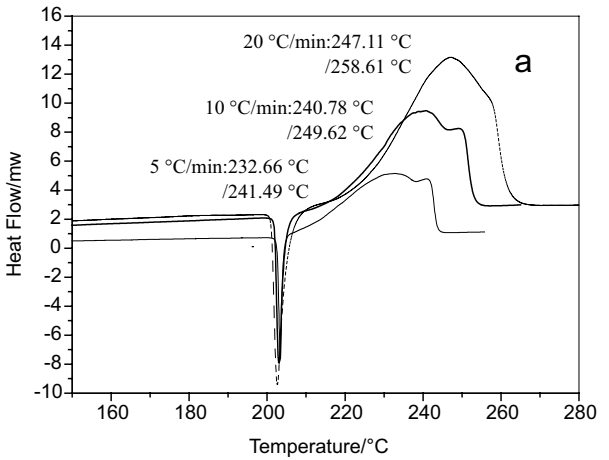

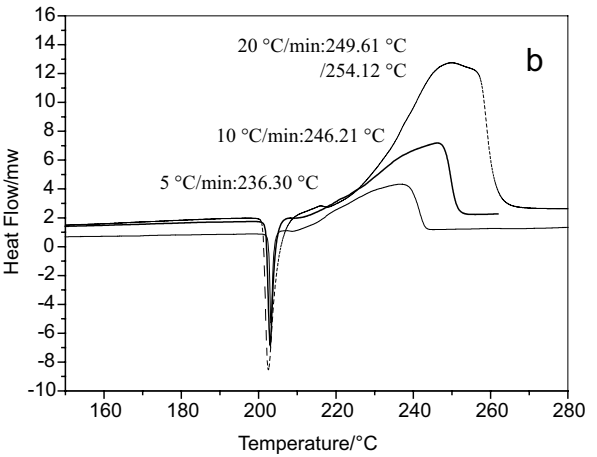

Figure 5. DSC thermographs of RDX and the mixture of RDX with Al nanoparticles.

Figure 5 shows that both pure RDX and mixtures of RDX with Al nanoparticles exhibit a sharp endothermic peak at the aroud 204 °C (Lit. 205.3 °C [23]), which suggests that the Al nanoparticles have no effect on the melting temperature of RDX. Pure RDX, at all three heating rates, exhibits two exothermic peaks, the first peak being attributed to the cleavage of N-N bonds, and the latter peak to the cleavage of C-N bonds. The peak temperatures increased with heating rate. By contrast, only one exothermic peak is observed in the DSC curves of the mixture of RDX with Al nanoparticles. This result indicates that the two peaks for RDX are combined into one exothermic peak by the Al nanoparticles. The peak temperatures from the mixture of RDX with Al nanoparticles at different heating rates decreased by about 4.36 °C, indicating that the Al nanoparticles affect the decomposition of RDX.

Thermal kinetic parameters

The decomposition kinetic parameters for RDX and for the mixture of RDX with Al nanoparticles were determined via the Kissinger Equation (Eq. 2), in order to study the effect of the Al nanoparticles on the kinetics of RDX thermal decomposition [24].

$$\ln\frac{\beta_i}{T_{pi}^2} = \ln\frac{A\,R}{E} - \frac{E}{RT_{pi}} \tag{2}$$

where β_i is the heating rate in K·min^{-1}; T_{pi} is the peak decomposition temperature

at β_i in K; A is the pre-exponential factor; E is the activation energy in J·mol^{-1}; R is the universal gas constant, 8.314 J·mol^{-1}·K^{-1}.

For Eq. 2, a straight line is obtained when $ln(\beta_i/T^2)$ is plotted against $1/T_{pi}$, and is shown in Figure 6. The activation energy (E_a) and the frequency factor (A) of the samples was calculated from the slope $-E/R$ and the intercept $ln(AR/E)$.

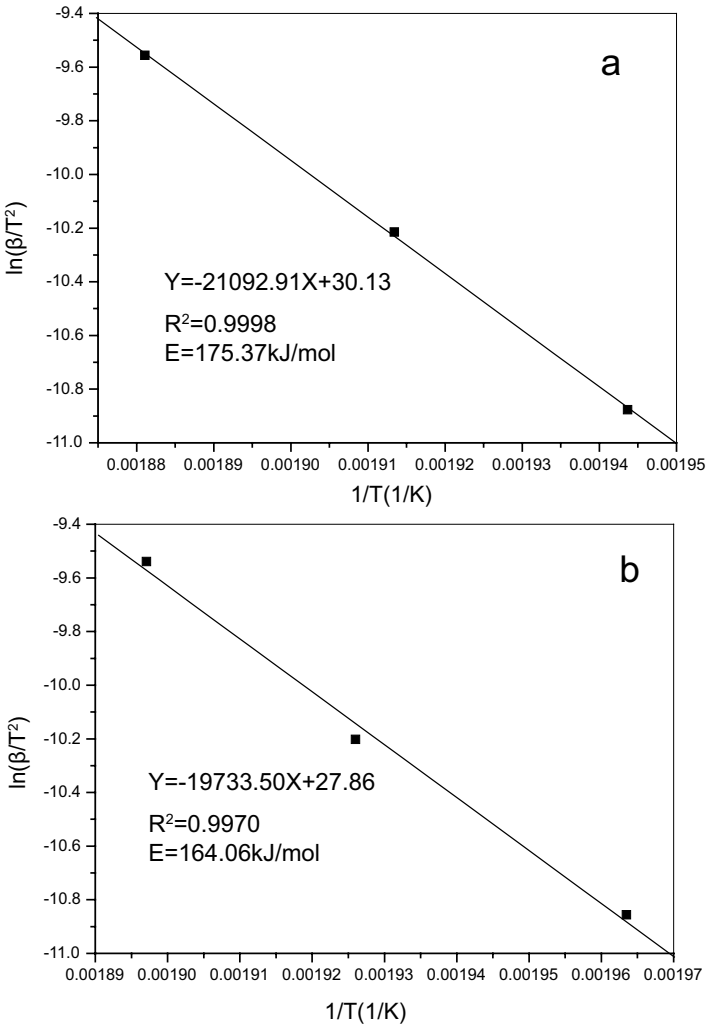

Figure 6. Kissinger's plots of ln (β_i/T^2) versus reciprocal peak temperature 1/T for RDX and for the mixture of RDX with Al nanoparticles. Symbol R is used to identify the linear correlation coefficient of ln (β_i/T^2) to 1/T. (a) RDX; (b) mixture of RDX with Al nanoparticles.

Figure 6 shows that the plots of ln (β_i/T^2) against 1/T for the two samples are both linear with a high linear correlation coefficient (R). Thus, Kissinger's kinetic model provides a good description of the overall, observed decomposition behavior in this temperature range. The activation energy for RDX and that of the mixture of RDX with Al nanoparticles is 175.37 (±3.64) kJ/mol and 164.06 (±12.84) kJ/mol, respectively. These results indicate that the activation energy for RDX decomposition is lowered about 11 kJ/mol by the Al nanoparticles.

Critical explosion temperature

The critical explosion temperature (T_b) can express the difficulty of initiating an explosion by thermal stimulus, and was evaluated using Eqs. 3 and 4 [25, 26].

$$T_e = T_{pi} - b\beta_i - c\beta_i^2 \tag{3}$$

$$T_b = \frac{E - \sqrt{E^2 - 4RET_e}}{2R} \tag{4}$$

where β_i is the heating rate in K·min^{-1}; T_{pi} is the peak temperature of decomposition at β_i in K; T_e is the peak temperature when β_i is zero in K; b and c are constants; T_b is the critical explosion temperature in K; E is the activation energy in J·mol^{-1}; and R is the universal gas constant, 8.314 J·mol^{-1}·K^{-1}.

Based on these equations, T_b of RDX was decreased from 516.7 K to 508.7 K by adding Al nanoparticles, indicating that Al nanoparticles cause RDX to decompose at a lower temperature.

The above results indicate that the peak temperature, the activation energy, and the critical explosion temperature of RDX are all decreased by the addition of Al nanoparticles. These results are reasonable, considering that the huge specific surface area and the potential high surface energy can give rise to high catalytic activity.

Conclusions

(1) Particles of nano-Al having a smooth surface were prepared by the DC arc plasma method. The median particle size of the nanoparticles was about 60 nm.

(2) The Al nanoparticles catalyse the thermal decomposition of RDX. The peak temperature for RDX decomposition is decreased by 4.36 K at different heating rates (5, 10, and 20 K/min) after the addition of nano-Al powder.

Moreover, the activation energy and the critical temperature for thermal explosion were decreased by 11kJ/mol and 8.0 K, respectively.

References

[1] Pantoya M., Granier,J., Combustion Behavior of Highly Energetic Thermites: Nano versus Micron Composites, *Propellants Explos. Pyrotech.*, **2005**, *30*(1), 53-62.
[2] Tillotson T.M., Gash A.E, Simpson R.L, Hrubesh L.W, Satcher J.H, Poco J.F., Nanostructured Energetic Materials using Sol-Gel Methodologies, *J. Non-Cryst. Solids*, **2001**, *285*(1-3), 338-345.
[3] Yang G., Nie F., Huang H., Zhao L., Pang W., Preparation and Characterization of Nano-TATB Explosive, *Propellants Explos, Pyrotech.*, **2006**, *31*(5), 390-394.
[4] Davin P.G., Klapötke T.M., Nanoscale Aluminum − Metal Oxide (Thermite) Reactions for Application in Energetic Materials, *Cent. Eur. J. Energ. Mater.*, **2010**, *7*(2), 115-129.
[5] Armstrong R.W., Baschung B., Booth D.W., Samirant M., Enhanced Propellant Combustion with Nanoparticles, *Nano Lett.*, **2003**, *3*(2), 253-255.
[6] Sathiskumar P.S., Thomas C.R., Giridhar Madras, Solution Combustion Synthesis of Nanosized Copper Chromite and its Use as Burn Rate Modifier in Solid Propellants, *Ind. Eng. Chem. Res.*, **2012**, *51*(30), 10108-10116.
[7] Kanel G.I., Utkin A.V., Razzorenov S.V., Rate of the Energy Release in High Explosives Containing Nano-size Boron Particles, *Cent. Eur. J. Energ. Mater.,* **2009**, *6*(1), 15-30.
[8] Ma Z., Li F., Bai H., Effect of Fe_2O_3 in Fe_2O_3/AP Composite Particles on Thermal Decomposition of AP and on Burning Rate of the Composite Propellant. *Propellants Explos. Pyrotech.*, **2006**, *31*(6), 447-451.
[9] Wang Y.P, Zhu J.W., Yang X.J., Lu L.D., Wang X., Preparation of NiO Nanoparticles and Their Catalytic Activity in the Thermal Decomposition of Ammonium Perchlorate, *Thermochim. Acta,* **2005**, *437*(1-2), 106-109.
[10] Shen S.M., Chen S.. Wu B.H., The Thermal Decomposition of Ammonium Perchlorate (AP) Containing a Burning Rate Modifier, *Thermochim. Acta,* **1993**, *223*(1), 135-143.
[11] Liu L., Li F., Tan L., Ming L., Yi Y., Effects of Nanometer Ni, Cu, Al and NiCu Powders on the Thermal Decomposition of Ammonium Perchlorate, *Propellants Explos, Pyrotech.*, **2004**, *29*(1), 34-38.
[12] Teipel U., *Energetic Materials: Particle Processing and Characterization*, Wiley-VCH , Weinheim, **2006**, pp. 267-270.
[13] Mostert F.J., Toit C., Measuring the Blast Output of Aluminized Explosive Charges in a Semi-Confined Environment, *Insensitive Munitions & Energetic Materials Technology Symposium*, Munich, Germany, October 11-14, **2010**, 1-8.
[14] Florczak B., A Comparison of Properties of Aluminized Composite Propellants

Containing HMX and FOX-7, *Cent. Eur. J. Energ. Mater.*, **2008**, *5*(3-4), 103-111.
[15] Gogulya M.F., Makhov M.N. , Dolgoborodov A.Y., Brazhnikov M.A., Arkhipov V.I., Shchetinin V.G., Mechanical Sensitivity and Detonation Parameters of Aluminized Explosives, *Combust., Explos. Shock Waves (Eng. Transl.)*, **2004**, *40*(4), 445-457.
[16] Reshetov A.A., Shneider V.B., Yavorovsk N.A., Ultradispersed Aluminum's Influence on the Speed of Detonation of Hexogen, Mendeleev All-Union Society Abstracts, 1, **1984**.
[17] Ivanov Y.F., Osmonoliev M.N., Sedoi V.S., Arkhipov, V.A., Bondarchuk S.S., Vorozhtsov A.B., Korotkikh A.G., Kuznetsov V.T., Productions of Ultra-Fine Powders and Their Use in High Energetic Compositions, *Propellants Explos. Pyrotech.*, **2003**, *28*(6), 319-333.
[18] Mench M.M., Kuo K.K., Yeh C.L., Lu Y.C, Comparison of Thermal Behavior of Regular and Ultra-Fine Aluminum Powders (Alex) Made from Plasma Explosion Process, *Comb. Sci. Tech,* **1998**, *135*(1-6), 269-292.
[19] Jones D.E.G., Brousseau P., Fouchard R.C., Turcotte A.M., Kwok Q.S.M, Thermal Characterization of Passivated Nanometer Size Aluminum Powders, *J. Therm. Anal. Calorim.,* **2000**, *61*(3), 805-818.
[20] Brousseau P., Anderson J.C., Nanometric Aluminum in Explosives, *Propellants Explos. Pyrotech.*, **2002**, *27*(5), 300-306.
[21] Weibel A., Bouchet R., Boulc'h F., Knauth P., The Big Problem of Small Particles: A Comparison of Methods for Determination of Particle Size in Nanocrystalline Anatase Powders, *Chem. Mater.*, **2005**, *17*(9), 2378-2385.
[22] Patterson A.L., The Scherrer Formula for X-Ray Particle Size Determination, *Phys. Rev.,* **1939**, *56*(10), 978-982.
[23] McKenney R.L., Krawietz J.T.R., Binary Phase Diagram Series: HMX/RDX, *J. Energ. Mater.,* **2003**, *21*(3), 141-166.
[24] Kissinger H.E., Reaction Kinetics in Differential Thermal Analysis, *Anal. Chem.* **1957**, *29*(11), 1702-1706.
[25] Zhang T.L., Hu R.Z., Xie Y., Li F.P., The Estimation of Critical Temperatures of Thermal Explosion for Energetic Materials using Non-isothermal DSC, *Thermochim. Acta,* **1994**, *244*(1), 171-176.
[26] Sovizi M.R., Hajimirsadeghi S.S., Naderizadeh B., Effect of Particle Size on Thermal Decomposition of Nitrocellulose, *J. Hazard. Mater.*, **2009**, *168*(2-3), 1134-1139.